Acta Geochim (2018) 37(2):323–333
https://doi.org/10.1007/s11631-017-0228-5

ORIGINAL ARTICLE

Re–Os geochronology of the Cambrian stage-2 and -3 boundary in Zhijin County, Guizhou Province, China

Shuaichao Wei[1] · **Yong Fu**[1,2] · **Houpeng Liang**[1] · **Zhihua Ge**[1] · **Wenxi Zhou**[1] · **Guangzhe Wang**[3]

Received: 5 April 2017 / Revised: 28 June 2017 / Accepted: 16 August 2017 / Published online: 5 September 2017

Abstract The black shale series that formed in the Ediacaran–Cambrian transition are important stratigraphic records of the co-evolution of the paleo-ocean, -climate, and -biology. In this study, we measured Re–Os isotopic compositions of the black shale in the Niutitang Formation from the Gezhongwu section in Zhijin, Guizhou Province. The samples had high Re and Os contents, with Re ranging from 21.27 to 312.78 ng/g and Os ranging from 0.455 to 7.789 ng/g. The Re–Os isotope isochron age of 522.9 ± 8.6 Ma implies deposition of the Niutitang black shale predated the Chengjiang Fauna, providing an age constraint for the expansion of oceanic anoxia in the study area. The initial $^{187}Os/^{188}Os$ ratio of 0.826 ± 0.026 indicates that enhanced continental weathering might have triggered the expansion of the oceanic anoxia.

Keywords Ediacaran–Cambrian transition · Black shale · Re–Os isochron age · Initial ratio

The Ediacaran-Cambrian (E–C) transition is an important interval in geological history. During this interval, Ediacaran soft-body biota were replaced by small shelly fossils (SSFs), after which occurred the major phase of the "Cambrian Explosion," regionally evidenced by the Chengjiang Biota (Hou et al. 2004; Zhu 2010). The Global Boundary Stratotype Section and Point (GSSP) E–C boundary is marked by the first appearance of trace fossil *Treptichnus pedum*, or by SSFs in the platform facies of the Yangtze Block (Brasier et al. 1994; Landing 1994; Buatois et al. 2013). Currently, the first occurrence of SSFs has been constrained by a zircon U–Pb age of 539.4 ± 2.5 Ma from bentonite (Compston et al. 2008), but their extinction time remains controversial. Meanwhile there is only a rough estimated age of 525 Ma for the Chengjiang Biota (Zhu et al. 2003). Therefore, a reliable radiometric age of the Chengjiang Biota was sought in this study. Furthermore, the oceanic anoxic event (OAE), formed by the expansion and/or intensification of the global or local anoxic ocean waters during a relatively short time interval, occurred globally during the E–C transition, having great influence on the co-evolution of environment-life processes on Earth's surface. Hence, the timing of the OAE is crucial to the understanding of several problems.

In the past, multiple isotopic dating methods, such as Rb–Sr, K–Ar, Sm–Nd, and U–Pb dating, have been applied to constrain the depositional age of sedimentary strata (Dickin 2005), but these methods are limited by the availability of suitable dating materials. In contrast, the Re–Os dating methodology can be well-applied in organic-rich rocks, i.e., black shale, because these rocks are high in Re–Os. Because the closure temperature of the Re–Os isotopic system is relatively high (Dickin 2005; Li et al. 2014), with negligible diagenetic alteration, Re–Os has been widely used in dating sedimentary rocks (Cohen 2004; Hannah et al. 2004; Selby and Creaser 2005; Kendall et al. 2009; Li et al. 2014). On the other hand, the Os isotope is an effective tracer for the paleo-ocean environment, being particularly sensitive to hydrothermal activity (Cumming et al. 2012; Fu et al. 2016). In this study, we

✉ Yong Fu
byez1226@126.com

[1] School of Resources and Environments, Guizhou University, Guiyang 550025, Guizhou, China

[2] Institute of Mineral Resources, Chinese Academy of Geological Sciences, Beijing 100037, China

[3] State Key Laboratory of Biogeology and Environmental Geology, China University of Geosciences, Wuhan 430074, China

utilized the Re–Os isotopic system to investigate the black shale at the base of the Niutitang Formation from the Gezhongwu section in the Zhijin area, Guizhou Province. This paper aims to: (1) constrain the ages of OAE and of the subsequent occurrence of the Chengjiang Biota in the Early Cambrian using the Re–Os isochron age; (2) explore the environmental background of the Early Cambrian OAE and subsequent Cambrian Explosion in light of the initial Os isotopic ratios.

1 Geologic setting

From the Early Ediacaran, large-scale carbonate platform systems have been established on paleo-highs in the Yangtze Block (Jiang et al. 2009). However, in the late Ediacaran, enhanced extensional tectonism caused block tilting and differential subsidence across faulted blocks, resulting in intense subaerial exposure and erosion on the uplifted ridges of platforms, apparently forming an unconformity with respect to the overlying Lower Cambrian sediments. In subsequent large-scale transgression, the carbonate platforms were completely flooded or submerged, thereby forming a fine-grained siliciclastic shelf-basin setting (Yeasmin et al. 2016) (Fig. 1a, b). The study area thus experienced an environmental change from dolomitic-phosphatic shelf to fine-grained (muddy) siliciclastic shelf.

The Gezhongwu area, about 14 km east of Zhijin City, is located on the southeastern wing of the Dayuan anticline, across which the Ediacaran, Cambrian, Carboniferous, Permian, and Triassic systems crop out (Fig. 1c). The lithostratigraphic units of the Ediacaran and Lower Cambrian include the Dengying, Gezhongwu and Niutitang Formations, in ascending order (Fig. 2); simple descriptions are provided below.

2 Samples and methods

In view of the high Re and Os contents of black shale, samples were mainly selected from black (carbonaceous) shale in the lower part of the Niutitang Formation.

All samples were collected from a 2 m-thick drill core with sampling spacing of 10 cm, ensuring sufficient expansion of the Re–Os isochrones and a precise Re–Os isotopic age. To avoid potential diagenetic alteration, samples containing hydrothermal veins and pyrites were excluded.

The selected samples were carefully cleaned, then put in a drying oven for 24 h at a constant temperature of 60 °C. Bulk sample was grinded to 200 mesh using a mortar, and the mortar was carefully cleaned by alcohol between samples to avoid contamination. Approximately 0.5 g of sample powder was precisely weighed, and then transferred by neck funnel to a pipe with length 20 cm and diameter 2 cm at the bottom of the Carius. After using 3 mL 15-mol/L hydrochloric acid to transfer the ^{185}Re–^{190}Os mixed diluent into the Carius tube being frozen with liquid nitrogen, we added 5 mL 15-mol/L HNO_3 and 1 mL 30% H_2O_2. The Carius tube was heated at 230 °C for 24 h after being liquefied with petroleum gas and oxygen flame (Du et al. 2001; Qu and Du 2003). After reaction, we opened the frozen Carius tube at the narrow neck, added ultrapure water to 25 mL, and used 5 mL ultrapure water, the absorption solution, to separate and enrich the Os by direct distillation (Li et al. 2010). After completing the distillation of Os, we turn the distilled residue in the Carius tube into a 150-mL Teflon beaker, and put it on the heating plate until nearly dry. We used acetone to extract Re in 10-mol/L NaOH alkaline medium (Li et al. 2009). After acetone drying, we added 2 mL ultrapure water. Lastly, we used the X-series inductively coupled plasma–mass spectrometer (ICP-MS) to measure the isotopic ratio. Re and Os measurement accuracies were 0.1% and 0.5%, respectively.

3 Results

The Re–Os abundances and isotopic data for the Niutitang black shale are shown in Table 1. In this experiment, the blanks of Re and Os were -0.001 and 0.0002 ng/g, respectively—significantly lower than the Re and Os contents in samples, which ranged from 21.27 to 312.78 ng/g and from 0.455 to 7.789 ng/g, respectively. The ^{187}Re/^{188}Os ratio varied between 102.30 and 306.43, and the ^{187}Os/^{188}Os ratio between 1.72 and 3.51. Thus, even samples with lower Re and Os contents were not affected by the blanks. Thus, the errors of ^{187}Re/^{188}Os and ^{187}Os/^{188}Os ratios mainly derived from mass spectrometer, ratio of diluent, balanced reaction between diluent and sample, and reproducibility of sample data. The corrected data were analyzed by isoplot, generating a Re–Os isochron (Ludwig 2001) with a decay constant of 1.666×10^{-11} a^{-1} for ^{187}Re (Smoliar et al. 1996; Ludwig 1999, 2001). The Jinchuan standard samples from the Re–Os Laboratory of National Research Center were used as the standards in this study. The measured Re and Os contents were 39 and 16.49 ng/g, respectively, and the ratios of ^{187}Re/^{188}Os and ^{187}Os/^{188}Os were 12 and 0.338, respectively, consistent with the recommended ratios. The Re–Os isotope age of the black shale samples was 522.9 ± 8.6 Ma with initial ^{187}Os/^{188}Os of 0.826 ± 0.026 (MSWD = 0.52).

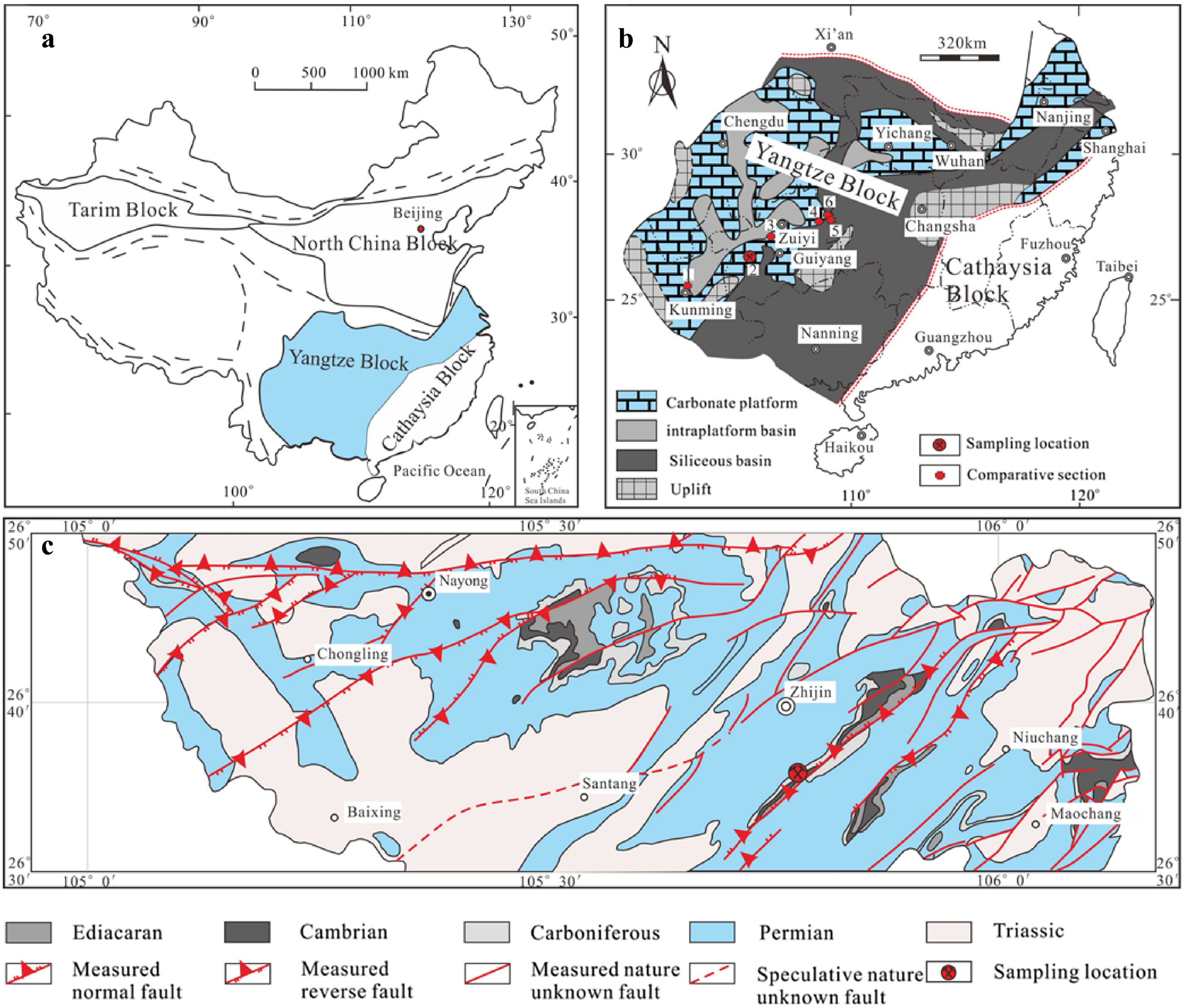

Fig. 1 **a** Geographic location of the Yangtze Platform; **b** paleogeographic map of the Yangtze Platform in the Early Cambrian (modified from Yeasmin et al. 2016); **c** geologic sketch map of Nayong-Zhijing in Guizhou. Note the sampling location

4 Discussion

4.1 Re–Os isotopic dating of black shale

The Re–Os isotopic system can effectively reflect the depositional age of black shale, and is mainly affected by two factors. The first is the sources of Re and Os in black shale. During the E–C transition, the global OAE (Leggett 1980; Wu et al. 1999, 2000) caused a rapid reduction of seawater Os. With the upward migration of the redox boundary, Re and Os oxides were reduced and entered into the organic phase via adsorption of organic matter and/or sulfide generated by reaction with H_2S. As a result, the Re–Os isotopic closed system was formed. Given the Re and Os contents of typical black shales in other ages (Fig. 3), we suggest that the Re and Os in the black shale derived from seawater.

The second factor is diagenetic alteration. (Creaser et al. 2002) suggested that the Re–Os isotope system in black shale could not be destroyed at temperatures as high as 650 °C as indicated by the simulation experiment. Therefore, the influence of regional tectonic metamorphism and hydrothermal activity would be negligible on the Re–Os system. Jiang and Li (2010) used the thermoelectric coefficient method of pyrite to obtain a formation temperature of 100–240 °C from the coarse-grained sulfide (pyrite) of the Lower Cambrian black shale series in the Tian'eshan section of Zunyi, Guizhou. In addition, the formation temperatures of fracture-filled quartz and calcite crystals in the black shales measured by the homogenization

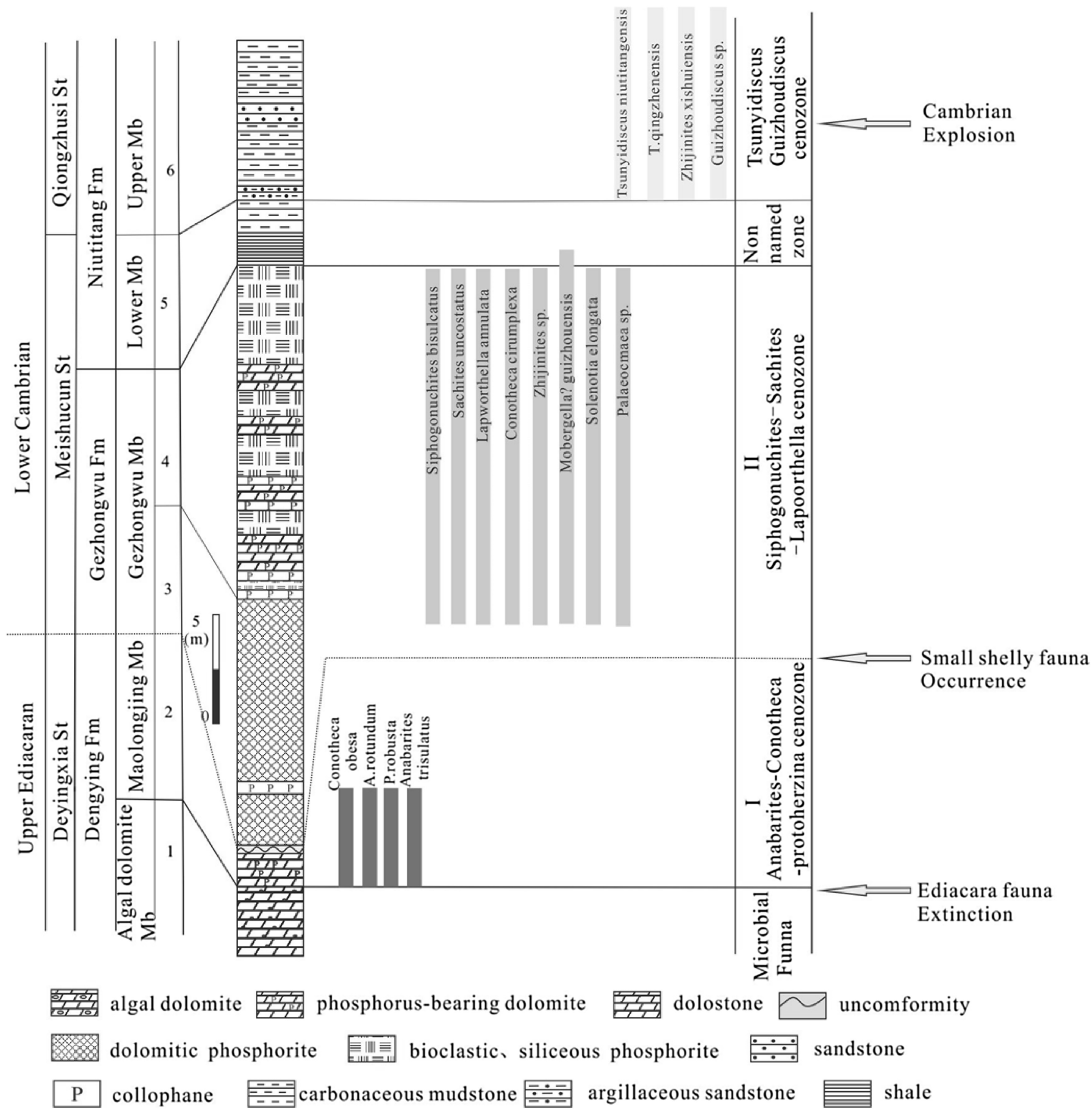

Fig. 2 Ediacaran–Cambrian boundary succession in the Gezhongwu section, Zhijin. (Niutitang Formation: *6*. *Dark gray* to *black* carbonaceous mudstones intercalated with siltstone layers. ~15 m thick. *5*. *Dark gray* to *black* mudstone/shale, containing siliceous–phosphatic concretions, and anomalously high concentrations of Mo, Ni, and V. ~15 m thick. Conformity. Gezhongwu Formation: *4*. *Dark purplish* medium-bedded dolomitic bioclastic phosphorite, siliceous phosphorite, and phosphatic dolostone intercalated with liver-colored cellophane. 12.8 m thick. *3*. Varicolored siliceous phosphorite with angular rubbles/breccias of dolostone, phosphorite, and chert. 11.6 m thick. Unconformity: Dengying Formation: *2*. Maolongjing Member: *light-gray* to *gray* thin-bedded phosphatic micro- to fine-crystalline dolostone. 2.6 m. *1*. Algae dolostone Member: *light-gray* to *gray* thin- to thick-bedded algal dolostone and laminated siliceous dolostone. 3.2 m thick. Base not observed.)

temperature of fluid inclusions were 126–230 °C and 113–153 °C, respectively. In this light, the diagenetic temperature was significantly lower than the disclosure temperature limit of the Re–Os system, suggesting that the isotopic system of the Zhijin samples was well preserved with a good closure, so that the Re–Os isochron age can effectively reflect the depositional age of black shales. Despite the existence of errors of instrument and technique, we believe the samples have the same initial isotopic composition.

Table 1 Re–Os abundances and isotope data

Sample	Category	Re ng/g	dRe	Os ng/g	dOs ng/g	$^{187}Re/^{188}Os$	2σ	$^{187}Os/^{188}Os$	2σ
zk2902-87	Black shale	29.29	0.22	0.626	0.006	225.84	2.80	2.81	0.03
zk2902-88		32.16	0.35	0.538	0.005	288.63	3.99	3.33	0.02
zk2902-89		21.27	0.18	0.546	0.006	188.26	2.56	2.49	0.03
zk2902-90		28.89	0.25	0.455	0.004	306.43	3.96	3.51	0.03
zk2902-100		135.67	1.10	2.615	0.027	250.60	3.31	3.02	0.03
zk2902-102		155.60	1.83	3.067	0.023	245.05	3.44	2.97	0.02
zk2902-103		312.78	2.49	7.789	0.083	193.96	2.57	2.53	0.03
zk2902-104		146.7	1.15	4.076	0.034	173.80	2.00	2.36	0.02
zk2902-106		90.4	0.70	3.227	0.026	135.37	1.53	2.01	0.01
zk2902-108		105.8	0.87	4.994	0.044	102.30	1.23	1.72	0.01
JCBY	Jinchuan standard	39.00	0.00	16.50	0.15	12.00	0.16	0.34	0.003
BK		−0.001	−0.0009	0.00021	0	−24	−36	1	2

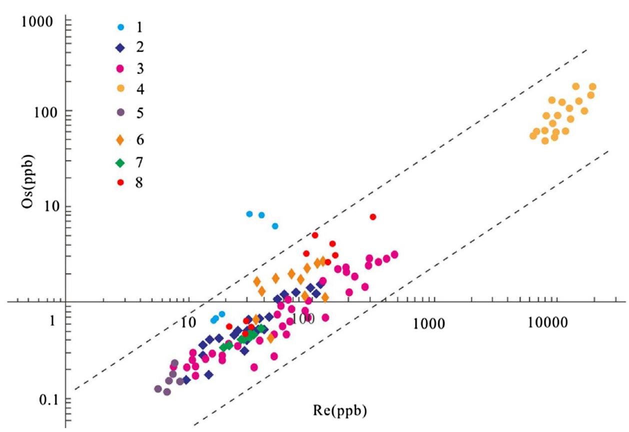

Fig. 3 Re–Os content of typical black shale in the world. *1*: Re–Os contents in pyrite in black shale in South Africa (Hannah et al. 2004); *2*: Re–Os contents in sedimentary rock of Mesoproterozoic in Taoudeni basin, Mauritania (Rooney et al. 2010); *3*: Re–Os contents in black shale in Britain (Cohen et al. 1999); *4*: Re–Os contents in metalliferous layer in Hunan and Guizhou Provinces (Fu et al. 2016); *5*: Re–Os contents of siliceous shale in Hunan and Guizhou Provinces (Fu et al. 2016); *6*: Re–Os contents of black shale in Hunan and Guizhou Provinces; *7*: Re–Os contents of Neoproterozoic black shale in the South of Australia and Northwest of Tasmania (Kendall et al. 2009). Data are from Cohen et al. 1999; Kendall et al. 2009; Hannah et al. 2004; Rooney et al. 2010

Previous Re–Os studies mainly focused on the poly-metalliferous layer in the Niutitang Formation. The poly-metalliferous layers have much higher Re and Os contents than organic-rich rocks (with Re content up to ppm level, and Os content of several hundred ppb) (Li et al. 2002; Mao et al. 2002; Xu et al. 2011).

In spite of relatively low Re and Os contents, black shale samples from the Gezhongwu section yield a good whole-rock Re–Os isochron age of 522.9 ± 8.6 Ma for the basal Niutitang Formation (Fig. 4a). Previous research has shown Re–Os isochron ages at the metalliferous layer in the basal Niutitang Formation in this area mainly concentrated in 542～521 Ma (Table 2). Because the isotopic age is mainly controlled by the two end-members on the isochrone, in order to further reduce the data error, this paper obtained an Re–Os isochron age (523 ± 6.5 Ma) of the metalliferous layer in the basal Niutitang Formation, which is consistent with the experimental results of Re–Os age (Fig. 4b). A tuff layer that is widely observed below the poly-metalliferous layer has yielded zircon U–Pb ages of 532.3–522.3 Ma (Jiang et al. 2009). The zircon U–Pb ages from a tuff bed in the Meishucun section in Yunnan Province, Bahuang, Panmen, and Taoying sections in Guizhou Province ranges from 526.5 to 522.3 Ma (Compston et al. 2008; Wang et al. 2012; Chen et al. 2015a). At Songlin, Zunyi, an identical tuffaceous layer yielded two different zircon U–Pb ages at 532.3 ± 0.7 Ma (Xu et al. 2011) and 518 ± 5 Ma (Zhou et al. 2008). Together with ages measured previously, the Re–Os isochron age obtained in this study (522.9 ± 8.6 Ma) provides another useful constraint on the formation time of the Niutitang black shale in the Zhijin area.

4.2 Constraints on biological evolution

The Meishucun section in Yunnan Province used to be the standard candidate of the Precambrian-Cambrian boundary in South China (Qian and He 1996; Zhang et al. 1997; Zhu et al. 2003). However, it has been abandoned due to the presence of an unconformity between the Zhujiaqing and Dengying Formations. Even so, the Lower Cambrian succession at this section is complete, including, in ascending order, the Meishucun Stage (equivalent to the Fortunian Stage and Stage 2 of the global Terreneuvian

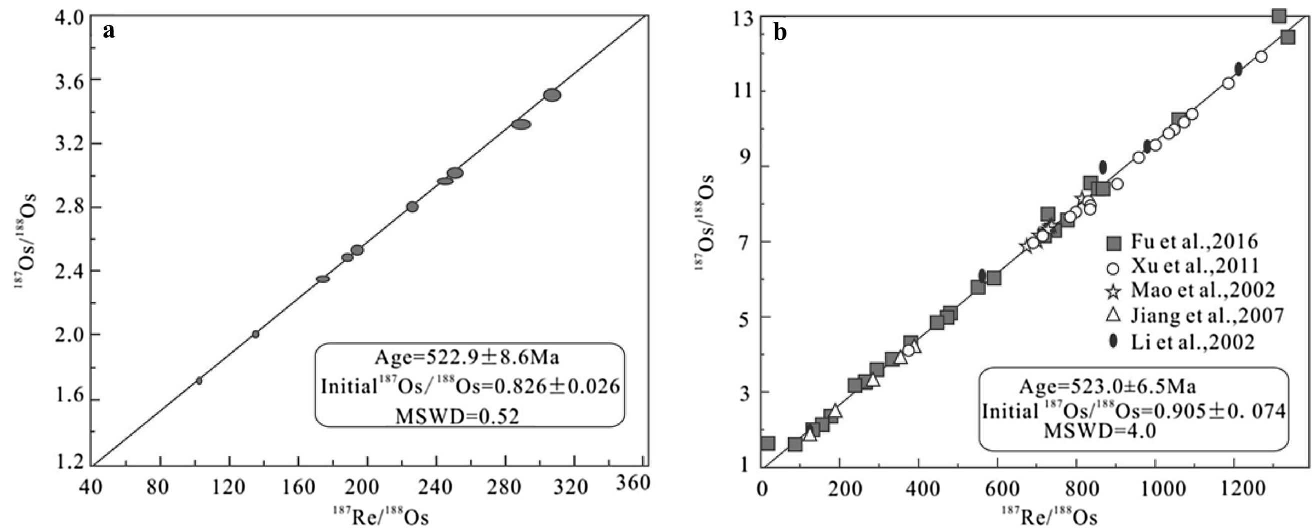

Fig. 4 **a** Re–Os isochron diagrams of black shale from the Niutitang Formation at Gezhongwu section in Zhijin; **b** Re–Os isochron diagrams of polymetallic sulfide bed from the Niutitang Formation in Guizhou and Hunan Provinces

Table 2 Re and Os isotope data of black shale in the Niutitang Formation in the Yangtze Platform

Sample	Sample number	$^{187}Re/^{188}Os$	$^{187}Os/^{188}Os$	Isochron age (Ma)	Initial ratio of Os	Source
Metalliferous deposits in Zunyi	6	122.9 ~ 387	1.9 ~ 4.2	535 ± 11	0.80 ± 0.04	Jiang et al. 2007
	10	673.2 ~ 813.2	6.8 ~ 8.1	541 ± 16	0.78 ± 0.19	Mao et al. 2002
	6	123.1 ~ 1211	6.1 ~ 65.2	542 ± 11	0.84 ± 0.12	Li et al. 2002
Metalliferous deposits in Guizhou and Hunan Provinces	24	6.88 ~ 1268	0.916 ~ 11.9	521 ± 5	0.87 ± 0.07	Xu et al. 2011
	28	86.6 ~ 1391	1.6 ~ 13	524.6 ± 4.8	0.88 ± 0.04	Fu et al. 2016
Black shale in Nayong	5	254 ~ 476	3.1 ~ 5.1	532 ± 14	0.85 ± 0.07	Fu et al. 2016
Black shale in Zhijin	10	102 ~ 306	1.72 ~ 3.5	522.9 ± 8.6	0.83 ± 0.02	This study

Series) and Qiongzhusi Stage (equivalent to Stage 3 of the global Series 2). The Meishucun Stage consists of the Zhujiaqing and Qiongzhusi (or Helinpu) Formations. Of these, the former includes, in ascending order, the Daibu (DB), Zhongyicun (ZYC), and Dahai (DH) members; the latter comprises the Shiyantou and Yuanshan members (Fig. 5).

There are four biostratigraphic marker levels (Fig. 5): Marker A, at the base of Daibu Member, represents the first appearance of the SSFs above which the *Anabarites trisulcatus–Protohertzina anabarics* assemblage (zone SSF1) appears in bed 3 of the basal Zhongyicun Member. Marker B, representative of SSF flourishing, is marked by the occurrence of *Paragloborilus subglobsosus–Purella squamulosa* assemblage (zone SSF2) in the top part of Zhongyicun Member, and by a volcanic ash layer (bentonite) (bed 5). Marker B was formerly used as the lower boundary of the Cambrian in China, but after 2004, the International Commission on Stratigraphy accepted the new division standard of four series and ten stages in the Cambrian, moving the basal boundary of the Cambrian downward (Peng 2006). Marker C is at the boundary between the Dahai and Shiyantou members, and represents a sedimentary environmental change from shallow water carbonate platform to organic-rich fine-grained siliciclastic (muddy) shelf. A volcanic tuff-originated bentonite layer around Marker C (Zhang 1997) yielded a zircon U–Pb age of 526.5 ± 1.1 Ma (Compston et al. 2008). Marker D, 2.4 m above the base of the Yuanshan Member, marks the appearance of the earliest trilobites. A large number of fossils of Chengjiang Biota were found in the siltstone and mudstone in the middle part of the Yu'anshan Member or above Marker D (Chen et al. 1994, 1999; Shu et al. 1999; Steiner et al. 2001). The black shale at the base of the Yuanshan Member is rich in metals Cr, Ni, Mo, and V (Zhu et al. 2003).

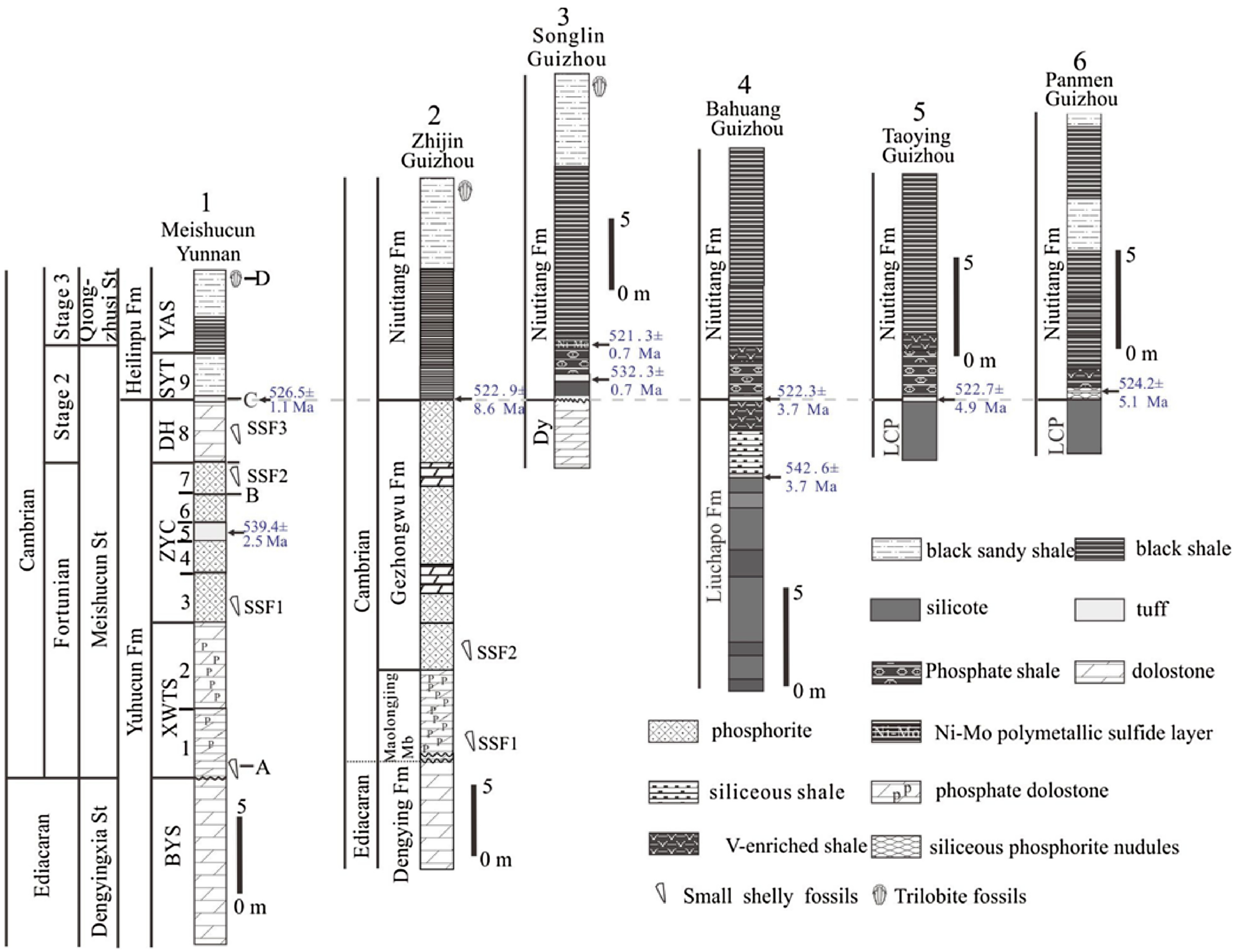

Fig. 5 Stratigraphic correlation of the E–C boundary successions between shallow- and deep-water settings in the Yangtze platform constrained by both U–Pb isotope ages and Re–Os isotope age data. (Meishucun section data from Compston et al. 2008; Songlin section data from Xu et al. 2011 (Re–Os) and Jiang et al. 2009 (U–Pb); Bahuang and Panmen data from Chen et al. 2015a; Taoying section data from Wang et al. 2012). *BYS* Baiyanshao, *XWTS* Xiaowaitoushan; *ZYC* Zhongyicun; *DH* Dahai; *SYT* Shiyantou; *YAS* Yuanshan; *LCP* Liuchapo; *DY* Dengying; *A*: SSF appearance; *B*: SSF biodiversity; *C*: sedimentary facies change point; SSF1: *Anabarites trisulcatus–Protohertzina anabarics* assemblage zone; SSF2: *Paragloborilus subglobsosus–Purella squamulosa* assemblage zone; SSF3: *Watsonella crosbyi* assemblage zone

The division of Sinian-Cambrian boundary strata is based on the type-section Meishucun, which corresponds with the Gezhongwu section in Zhijin. The two sections share a common fossil assemblage, SSF1: *Anabarites-Conotheca–Protohertzina* assemblage zone. However, due to environmental differences, different faunal members may exist in the same assemblage, i.e., in SSF2. It has been suggested that the *Siphogonuchites-Sachites–Lapworthella* assemblage zone at Gezhongwu is comparable to the *Paragloborilus subglobsosus–Purella squamulosa* assemblage zone in the Zhongyicun Member of the Yuhucun Formation in the Meishucun. In addition, few fossils occur in the lower Niutitang Formation at Gezhongwu, so it is debatable to some degree whether it correlates with the Heilinpu Formation of the Qiongzhusi Stage in the Meishucun section. Our Re–Os isochron age of the black shale at the base of Niutitang Formation (522.9 ± 8.6 Ma) corresponds (within the error range) with the zircon U–Pb age (526.5 ± 1.1 Ma; Compston et al. 2008) at the base of the Shiyantou Member of the Helingpu Formation.

4.3 Constraints on oceanic anoxic events

In South China, OAEs occurred from the Neoproterozoic to the Cambrian with a great thickness of black shales deposited. The changes in $\delta^{98/95}$Mo and δCe may reflect the occurrence of OAE (Fig. 6). Based on research by Wen et al. (2011), the maximum Mo isotopic ratio of euxinic sedimentary rock may approximately represent the lower limit of seawater Mo isotopic ratio, and the Mo isotopic composition of seawater is affected by the oxic sediments in the seafloor, which are dominantly controlled by

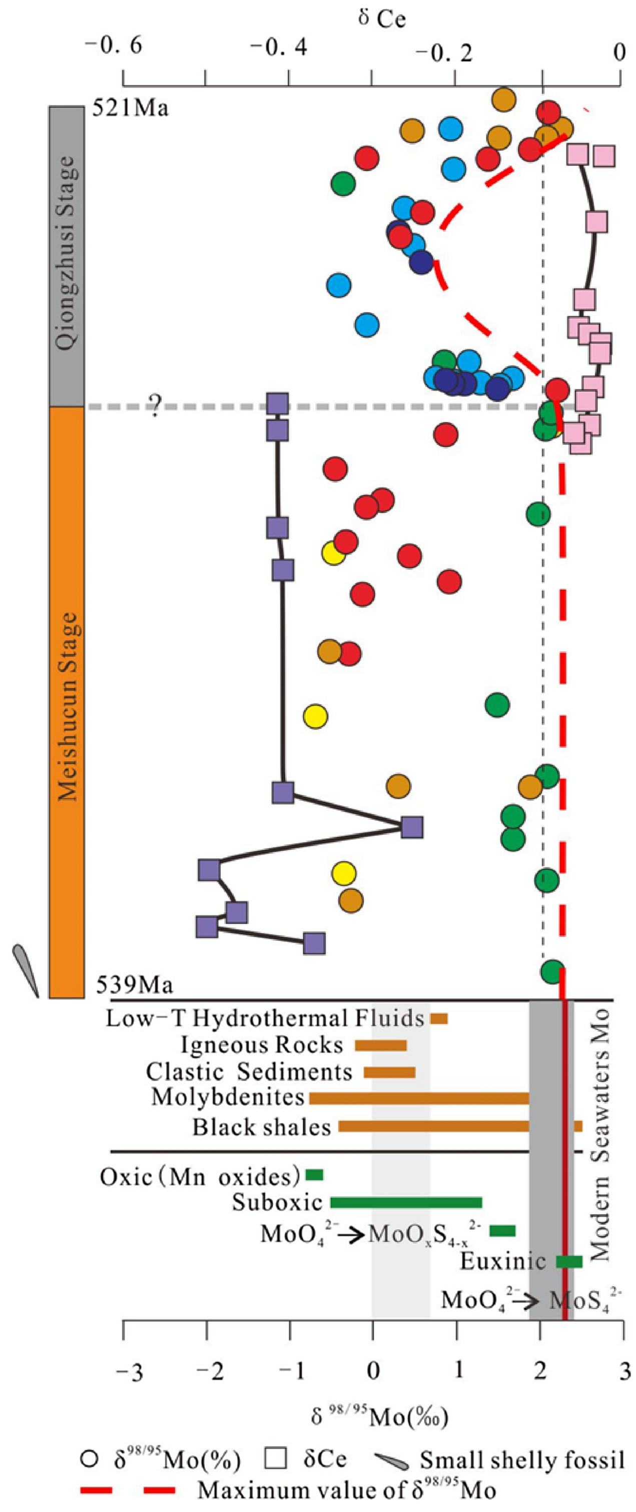

Fig. 6 Mo isotope and δCe variations in the Early Cambrian. Molybdenum isotope composition of modern seawaters derived from Kendall et al. (2009) and Xu et al. (2012). Colored circles represent different data sources (Lehmann et al. 2007; Xu and Lehmann 2010; Wen et al. 2011; Xu et al. 2012; Chen et al. 2015b; Mao 2015; Gao et al. 2016), similar to rectangle patterns

atmospheric oxygen and the redox conditions of the ocean (Anbar and Rouxel 2007). In addition, the cerium anomaly (δCe) can also be used as a tracer of paleo-environment (Wright et al. 1987). Generally, $\delta Ce < -0.1$ reflects oxic aqueous conditions, while $\delta Ce > -0.1$ reflects a reducing (or anoxic) condition (Wright et al. 1987). Through compiling $\delta^{98/95}$Mo and δCe datasets of phosphorite in the Gezhongwu Formation of the Meishucun Stage and the black shale in the Niutitang Formation of the Qiongzhusi Stage in the Lower Cambrian (Fig. 6), we found that the maximum $\delta^{98/95}$Mo value of phosphorite approached the modern seawater Mo isotope value, but the maximum $\delta^{98/95}$Mo values at the base of overlying black shales showed a negative excursion and subsequent rapid increase. In addition, δCe values (<-0.1) in the phosphorites of the Gezhongwu Formation indicate an oxic environment. In contrast, the δCe values (>-0.1) in black shales of the Niutitang Formation suggest a reducing environment, constrained at 522.9 ± 8.6 Ma by Re–Os isochron dating.

5 Possible implication of the initial Os isotopic ratio

Through geologic time, silicate weathering could have influenced atmospheric CO_2 concentration, thereby changing the climate. Currently, the Sr isotope composition of seawater is a widely available tracer of riverine flux resulting from continental weathering relative to the hydrothermal flux into the ocean. The increase of $^{87}Sr/^{86}Sr$ could have resulted from terrestrial weathering and/or enhanced orogeny, but there is generally a lack of widespread diagenetic-resistant materials available for Sr isotope analysis (Blum and Erel 1995; Derry and France-Lanord 1996; Quade and Ojha 1997). Os isotopic composition of seawater provides an alternative signature to trace the continental flux relative to hydrothermal flux, particularly for organic-rich sediments (Pegram et al. 1992; Ravizza 1993; Peucker-Ehrenbrink et al. 1995; Oxburgh 1998; Reusch et al. 1998; Pegram and Turekian 1999).

In general, the Os isotopic ratio is controlled by the redox conditions of the medium and source of Os. Three main sources of Os in seawater include: (1) riverine input with a $^{187}Os/^{188}Os$ ratio of 0.3–1.54; (2) mid-ocean ridge hydrothermal fluid with a $^{187}Os/^{188}Os$ ratio of about 0.12, and with a non-radioactive characteristic (Sharma et al. 2000); and (3) cosmic dust, having a comparable $^{187}Os/^{188}Os$ ratio to the mantle (Yang et al. 2005). The annual extraterrestrial Os supply is generally less than 17 kg (Levasseur et al.1999), accounting for quite a small part of the equivalent terrigenous supply. So the extrater-

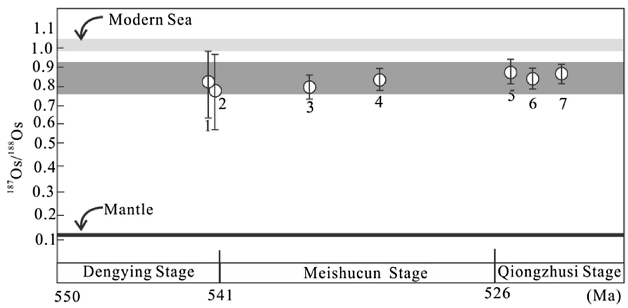

Fig. 7 Initial $^{187}Os/^{188}Os$ ratios of black shale in Early Cambrian, South China. *1*) Ni–Mo metalliferous deposits in Zunyi and Zhangjiajie area (Li et al. 2002); *2*) Ni–Mo metalliferous deposits in Zunyi (Mao et al. 2002); *3*) metalliferous deposits in Dayong in Hunan Province (Jiang et al. 2003); *4*) black shale under metalliferous deposits in Nayong (Fu et al. 2016); *5*) metalliferous deposits in Hunan and Guizhou Province (Fu et al. 2016); *6*) this study; *7*) Hunan and Guizhou Provinces (Xu et al. 2011)

restrial input is not a significant source of Os in the ocean. In fact, cosmic dust could even be adsorbed in the submarine Fe–Mn crust, decreasing the Os isotopic ratio of the Fe–Mn crust (Peucker-Ehrenbrink 1996; Burton et al. 1999; Sun et al. 2006). The modern ocean yields a $^{187}Os/^{188}Os$ ratio of 1.05–1.06, indicating mixing of different materials in seawater (Levasseur et al. 1999).

In this study, the initial $^{187}Os/^{188}Os$ ratio from the basal black shale of the Niutitang Formation in the Zhijin area was 0.826 ± 0.026 (Table 1; Fig. 7), falling within the range of 0.78–0.88 reported by other researchers (Li et al. 2002; Mao et al. 2002; Jiang et al. 2007; Xu et al. 2011; Fu et al. 2016), but slightly lower than that of a continental source. This indicates that the shale was deposited in the shelf sea affected strongly by continental weathering flux and somewhat by hydrothermal flux during the Early Cambrian (Qiongzhusi epoch), resulting in the moderately high radioactive Os in the seawater.

During the Qiongzhusi epoch, owing to huge amounts of greenhouse gas released by seafloor hydrothermal venting or volcanic activity, atmospheric CO_2 may have increased rapidly, causing climate warming. On the other hand, the warm climate may have facilitated a large-scale sea-level rise, leading to the widespread transgression and marine anoxia under which organic-rich sediments could have been deposited as seen the widespread (basin-scale) Niutitang black shales over the antecedent Yangtze carbonate platform.

6 Conclusion

This study carried out Re–Os isotopic dating for the black shale in the Niutitang Formation at Gezhongwu, Guizhou and yielded an isochron age of 522.9 ± 8.6 Ma, providing a radiometric time constraint on the onset of the Niutitang Formation and further facilitating stratigraphic correlation with the type section of E–C boundary strata in eastern Yunnan and elsewhere.

The initial Os isotope ratio of seawater during deposition of the Niutitang black shale was determined to be 0.826 ± 0.026, suggesting moderately strong continental weathering flux and likely submarine hydrothermal release into the seawater.

Acknowledgements This research was supported by the China Geological Survey (DD20160346), the National Natural Science Foundation of China (41472089) and the Guizhou Geological Prospecting Fund (2016091). We would like to thank Prof. Daizhao Chen for his valuable reviews, the anonymous reviewers and the editor for their constructive comments.

References

Anbar AD, Rouxel O (2007) Metal stable isotopes in paleoceanography. Annu Rev Earth Planet Sci 35(1):717–746

Blum JD, Erel Y (1995) A silicate weathering mechanism linking increase in marine $^{87}Sr/^{86}Sr$ with global glaciation. Nature 373:415–418

Brasier M, Cowie J, Taylor M (1994) Decision on the Precambrian-Cambrian boundary stratotype. Episodes 17:3–8

Buatois LA, Almond J, Germs GJB (2013) Environmental tolerance and range offset of *Treptichnus pedum*: implications for the recognition of the Ediacaran–Cambrian boundary. Geology 41:519–522

Burton KW, Bourdon B, Birck JL, Allègre CJ, Hein JR (1999) Osmium isotope variations in the oceans recorded by Fe–Mn crusts. Earth Planet Sci Lett 171:185–197

Chen JY, Ramskold L, Zhou GQ (1994) Evidence for monophyly and arthropod affinity of Cambrian giant predators. Science 264:1304–1308

Chen JY, Huang DY, Li CW (1999) An Early Cambrian craniate-like chordate. Nature 402:518–522

Chen D, Zhou X, Fu Y, Wang J, Yan D (2015a) New U–Pb zircon ages of the Ediacaran–Cambrian boundary strata in South China. Terra Nova 27:62–68

Chen X, Ling HF, Vance D, Shields-Zhou GA, Zhu MY, Poulton SW, Och LM, Jiang SY, Cremonese L, Archer C (2015b) Rise to modern levels of ocean oxygenation coincided with the Cambrian radiation of animals. Nat Commun 6:1–7

Cohen AS (2004) The rhenium–osmium isotope system: applications to geochronological and palaeoenvironmental problems. J Geol Soc 161:729–734

Cohen AS, Coe AL, Bartlett JM, Hawkesworth CJ (1999) Precise Re-Os ages of organic-rich mudrocks and the Os isotope composition of Jurassic seawater. Earth Planet Sci Lett 167:159–173

Compston W, Zhang Z, Cooper JA, Ma G, Jenkins RJF (2008) Further SHRIMP geochronology on the Early Cambrian of South China. Am J Sci 308:399–420

Creaser RA, Sannigrahi P, Chacko T, Selby D (2002) Further evaluation of the Re–Os geochronometer in organic-rich sedimentary rocks: a test of hydrocarbon maturation effects in the Exshaw Formation, Western Canada Sedimentary Basin. Geochim Cosmochim Acta 66:3441–3452

Cumming VM, Selby D, Lillis PG (2012) Re–Os geochronology of the lacustrine Green River Formation: insights into direct depositional dating of lacustrine successions, Re–Os systematics and paleocontinental weathering. Earth Planet Sci Lett 359–360:194–205

Derry LA, France Lanord C (1996) Neogene Himalayan weathering history and river $^{87}Sr/^{86}Sr$: impact on the marine Sr record. Earth Planet Sci Lett 142:59–74

Dickin AP (2005) Radiogenic isotope geology. Cambridge University Press, Cambridge, pp 42–286

Du AD, Zhao DM, Wang SX (2001) Precise Re–Os dating for molybdenite by ID-NTIMS with carius tube sample preparation. Rock Miner Anal 20:247–252

Fu Y, Dong L, Li C, Q WJ, Pei HX, Qiao WL, Shen B (2016) New Re–Os isotopic constrains on the formation of the metalliferous deposits of the Lower Cambrian niutitang formation. J Earth Sci 27:271–281

Gao P, Liu G, Jia C, Young A, Wang Z, Wang T, Zhang P, Wang D (2016) Redox variations and organic matter accumulation on the Yangtze carbonate platform during late Ediacaran–Early Cambrian: constraints from petrology and geochemistry. Palaeogeogr Palaeoclimatol Palaeoecol 450:91–110

Hannah JL, Bekker A, Stein HJ, Markey RJ, Holland HD (2004) Primitive Os and 2316 Ma age for marine shale: implications for Paleoproterozoic glacial events and the rise of atmospheric oxygen. Earth Planet Sci Lett 225:43–52

Hou XG, Aldridge RJ, Bergström J, Siveter DJ, Feng XH (2004) The Cambrian fossils of Chengjiang, China: the flowering of early animal life. Blackwell, Oxford, pp 1–233

Jiang YH, Li SR (2010) The genesis of pyrite from Ni–Mo deposit in the Lower Cambrian black rock series of Hunan and Guizhou provinces, China. Geol Bull Chin 29(2/3):427–435

Jiang SY, Yang JH, Ling HF, Feng HZ, Chen YQ, Chen JH (2003) Re-Os isotopes and PGE geochemistry of black shales and intercalated Ni-Mo polymetallic sulfide bed from the Lower Cambrian Niutitang Formation, South China. Prog Nat Sci Mater Int 13(10):788–794

Jiang SY, Yang JH, Ling HF, Chen YQ, Feng HZ, Zhao KD, Ni P (2007) Extreme enrichment of polymetallic Ni–Mo–PGE–Au in Lower Cambrian black shales of South China: an Os isotope and PGE geochemical investigation. Palaeogeogr Palaeclimatol Palaeoecol 254:217–228

Jiang SY, Pi DH, Heubeck C, Frimmel H, Liu YP, Deng HL, Ling HF, Yang JH (2009) Early Cambrian ocean anoxia in South China. Nature 459:E5–E6

Kendall B, Creaser RA, Gordon GW, Anbar AD (2009) Re–Os and Mo isotope systematics of black shales from the Middle Proterozoic Velkerri and Wollogorang Formations, McArthur Basin, northern Australia. Geochim Cosmochim Acta 73:2534–2558

Landing E (1994) Precambrian-Cambrian boundary global stratotype ratified and a new perspective of Cambrian time. Geology 22:179

Leggett JK (1980) The sedimentological evolution of a Lower Palaeozoic accretionary fore-arc in the Southern Uplands of Scotland. Sedimentology 27:401–417

Lehmann B, Nagler TF, Holland HD, Wille M, Mao JW, Pan JY, Ma DS, Dulski P (2007) Highly metalliferous carbonaceous shale and Early Cambrian seawater. Geology 35:403–406

Levasseur S, Birck JL, Allègre CJ (1999) The osmium riverine flux and the oceanic mass balance of osmium. Earth Planet Sci Lett 174:7–23

Li SR, Xiao QY, Shen JF, Sun L, Liu B, Yan BK (2002) Source of PGE and Re–Os isotopes restriction of ore age in the Lower Cambrian black shale series in Hunan and Guizhou provinces. Sci China Earth Sci 37:568–575

Li C, Qu WJ, Du AD, Sun WJ (2009) Comprehensive study on extraction of with acetone in Re–Os isotopic dating. Rock Miner Anal 28:233–238

Li C, Qu WJ, Zhou LM, Du AD (2010) Rapid separation of osmium by direct distillation with Carius tube. Rock Miner Anal 29(1):14–16

Li C, Qu WJ, Wang DH, Zhou LM, Du AD, Fu Y, Pei HX (2014) The progress of applying Re–Os isotope to dating of organic-rich sedimentary rocks and reconstruction of palaeoenvironment. Acta Geosci Sin 35:405–414

Ludwig KR (1999) Isoplot-A plotting and regression program for radiogenic-isoplot date. U S Geological Survey, 1999 Version, Open-file Report 91-445

Ludwig KR (2001) A geochronological toolkit for microsoft excel. Berkeley Geochronology Center, Isoplot/Ex 2.49. Special Publication No 1a

Mao T (2015) The analysis of forming environment and ore-controlling factors of phosphorous deposits in the bottom of Lower Cambrian, Central Guizhou Province, China. A Dissertation Submitted to Guizhou University for Doctoral Degree 1–123

Mao JW, Lehmann B, Du AD, Zhang GD, Ma DS, Wang YT, Zeng MG, Kerrich R (2002) Re–Os dating of polymetallic Ni-Mo-PGE-Au mineralization in Lower Cambrian black shales of South China and its geologic significance. Econ Geol 97:1051–1061

Oxburgh R (1998) Variations in the osmium isotope composition of sea water over the past 200,000 years. Earth Planet Sci Lett 159:183–191

Pegram WJ, Turekian KK (1999) The osmium isotopic composition change of Cenozoic sea water as inferred from a deep-sea core corrected for meteoritic contributions. Geochim Cosmochim Acta 63:4053–4058

Pegram WJ, Krishnaswami S, Ravizza GE, Turekian KK (1992) The record of sea water $^{187}Os/^{186}Os$, variation through the Cenozoic. Earth Planet Sci Lett 113:569–576

Peng SC (2006) New global subdivision on Cambrian chronostratigraphy. Bull Chin Acad Sci 21:325–328

Peucker-Ehrenbrink B (1996) Accretion of extraterrestrial matter during the last 80 million years and its effect on the marine osmium isotope record. Geochim Cosmochim Acta 60:3187–3196

Peucker-Ehrenbrink B, Ravizza G, Hofmann AW (1995) The marine $^{187}Os/^{186}Os$ record of the past 80 million years. Earth Planet Sci Lett 130:155–167

Qian Y, He TG (1996) New investigation of Precambrian-Cambrian boundary sections in eastern Yunnan. Acta Micropalaeontol Sin 13:225–240

Qu WJ, Du AD (2003) Highly precise Re–Os dating of molybdenite by ICP-MS with Carius tube sample digestion. Rock Miner Anal 22:254–257

Quade J, Ojha TP (1997) The Late Neogene $^{87}Sr/^{86}Sr$ record of lowland Himalayan rivers. Science 276:1828–1831

Ravizza G (1993) Variations of the $^{187}Os/^{186}Os$ ratio of seawater over the past 28 million years as inferred from metalliferous carbonates. Earth Planet Sci Lett 118:335–348

Reusch DN, Ravizza G, Maasch KA, Wright JD (1998) Miocene seawater $^{187}Os/^{188}Os$ ratios inferred from metalliferous carbonates. Earth Planet Sci Lett 160:163–178

Rooney AD, Selby D, Houzay JP, Renne PR (2010) Re–Os geochronology of a Mesoproterozoic sedimentary succession, Taoudeni basin, Mauritania: implications for basin-wide correlations and Re–Os organic-rich sediments systematics. Earth Planet Sci Lett 289:486–496

Selby D, Creaser RA (2005) Direct radiometric dating of the Devonian–Mississippian time-scale boundary using the Re–Os black shale geochronometer. Geology 33:545–548

Sharma M, Wasserburg GJ, Hofmann AW, Butterfield DA (2000) Osmium isotopes in hydrothermal fluids from the Juan de Fuca Ridge. Earth Planet Sci Lett 179:139–152

Shu DG, Luo HL, Morris SC, Morris C, Zhang XL, Hu SX, Chen L, Han J, Zhu M, Li Y, Chen LZ (1999) Lower Cambrian vertebrates from south China. Nature 402:42–46

Smoliar MI, Walker RJ, Morgan JW (1996) Re–Os ages of Group IIA, IIIA, IVA, and IVB iron meteorites. Science 271:1099–1102

Steiner M, Wallis E, Erdtmann BD, Zhao Y, Yang R (2001) Submarine-hydrothermal exhalative ore layers in black shales from South China and associated fossils—insights into a Lower Cambrian facies and bio-evolution. Palaeogeogr Palaeoclimatol Palaeoecol 169:165–191

Sun XM, Xue T, He GW, Zhang M, Shi GY, Wang SW, Lu HF (2006) Platinum group elements(PGE) and Os isotopic geochemistry of ferromanganese crusts from Pacific Ocean seamounts and their constraints on genesis. Acta Pet Sin 22:3014–3026

Wang X, Shi X, Jiang G, Zhang W (2012) New U-Pb age from the basal Niutitang Formation in South China: implications for diachronous development and condensation of stratigraphic units across the Yangtze Platform at the Ediacaran–Cambrian Transition. J Asian Earth Sci 48:1–8

Wen HJ, Carignan J, Zhang YX, Fan HF, Cloquet C, Liu SR (2011) Molybdenum isotopic records across the Precambrian-Cambrian boundary. Geology 39(8):775–778

Wright J, Schrader H, Holser WT (1987) Paleoredox variations in ancient oceans recorded by rare-earth elements in fossil apatite. Geochim Cosmochim Acta 51:631–644

Wu CD (2000) Recovery of the paleoocean environment in the alternating epoch of Late Sinian and Early Cambrian in the west Hunan. Earth Sci Front s2:45–57

Wu CD, Yang CY, Chen QY (1999) The origin and geochemical characteritics of Upper Sinian in Lower Cambrian black shales in western Hunan. Acta Pet Miner 18:26–38

Xu LG, Lehmann B (2010) Mo and Mo stable isotope geochemistry: isotope system, analytical technique and applications to geology. Miner Depos 30:103–124

Xu L, Lehmann B, Mao J, Qu W, Du A (2011) Re–Os age of polymetallic Ni-Mo-PGE-Au mineralization in Early Cambrian blake shales of South China—a reassessment. Econ Geol 106:511–522

Xu L, Lehmann B, Mao J, Nägler TF, Neubert N, Böttcher ME, Escher P (2012) Mo isotope and trace element patterns of Lower Cambrian black shales in South China: multi-proxy constraints on the paleoenvironment. Chem Geol 318–319:45–59

Yang JH, Jiang SY, Ling HF, Chen YQ (2005) Re–Os isotope tracing and dating of black shales and oceanic anoxic events. Earth Sci Front 12:143–150

Yeasmin R, Chen D, Fu Y, Wang J, Guo Z, Guo C (2016) Climatic-oceanic forcing on the organic accumulation across the shelf during the Early Cambrian (Age 2 through 3) in the mid-upper Yangtze Block, NE Guizhou, South China. J Asian Earth Sci 134:365–386

Zhang WT (1997) Cambrian explosion and significance of the Changjiang Fauna. Earth Sci Front 4:117–121

Zhang JM, Li GX, Zhou CM (1997) Geochemistry of light colour clayrock layers from the Early Cambrian Meishucun Stage in eastern Yunnan and their geological significance. Acta Pet Sin 13:100–110

Zhou MZ, Luo TY, Li ZX, Zhao H, Long HS, Yang Y (2008) SHRIMP U–Pb zircon age of tuff at the bottom of the Lower Cambrian Niutitang Formation, Zunyi, South China. Chin Sci Bull 53:576–583

Zhu MY (2010) The origin and Cambrian explosion of animals: fossil evidences from China. Acta Palaeontol Sin 49:269–287

Zhu M, Zhang J, Steiner M, Yang A, Li G, Erdtmann BD (2003) Sinian-Cambrian stratigraphic framework for shallow-to deep-water environments of the Yangtze Platform: an integrated approach. Prog Nat Sci 13:951–960